Published in final edited form as:
Circulation. 2008 September 9; 118(11): 1123–1129. doi:10.1161/CIRCULATIONAHA.107.738013.

Dynamic Mechanism for Initiation of Ventricular Fibrillation In Vivo

Anna R.M. Gelzer, DVM[*], **Marcus L. Koller, MD**[*], **Niels F. Otani, PhD**, **Jeffrey J. Fox, PhD**, **Michael W. Enyeart, MS**, **Giles J. Hooker, PhD**, **Mark L. Riccio, MSEE**, **Carlo R. Bartoli, BS**, and **Robert F. Gilmour Jr, PhD**
Departments of Clinical Sciences (A.R.M.G.) and Biomedical Sciences (N.F.O., M.W.E., M.L.R., C.R.B., R.F.G.), College of Veterinary Medicine, and Department of Statistical Science (G.J.H.), Cornell University, Ithaca, NY; Department of Cardiology, Center of Cardiovascular Medicine, Bad-Neustadt, Germany (M.L.K.); and Gene Network Sciences, Ithaca, NY (J.J.F.)

Abstract

Background—Dynamically induced heterogeneities of repolarization may lead to wave-front destabilizations and initiation of ventricular fibrillation (VF). In a computer modeling study, we demonstrated that specific sequences of premature stimuli maximized dynamically induced spatial dispersion of refractoriness and predisposed the heart to the development of conduction block. The purpose of this study was to determine whether the computer model results pertained to the initiation of VF in dogs in vivo.

Methods and Results—Monophasic action potentials were recorded from right and left ventricular endocardium in anesthetized beagle dogs (n=11) in vivo. Restitution of action potential duration and conduction time and the effective refractory period after delivery of the basic stimulus (S_1) and each of 3 premature stimuli (S_2, S_3, S_4) were determined at baseline and during verapamil infusion. The effective refractory period data were used to determine the interstimulus intervals for a sequence of 4 premature stimuli ($S_2S_3S_4S_5$=CL_{VF}) for which the computer model predicted maximal spatial dispersion of refractoriness. Delivery of CL_{VF} was associated with discordant action potential duration alternans and induction of VF in all dogs. Verapamil decreased spatial dispersion of refractoriness by reducing action potential duration and conduction time restitution in a dose-dependent fashion, effects that were associated with reduced inducibility of VF with CL_{VF}.

Conclusion—Maximizing dynamically induced spatial dispersion of repolarization appears to be an effective method for inducing VF. Reducing spatial dispersion of refractoriness by modulating restitution parameters can have an antifibrillatory effect in vivo.

Keywords

electrophysiology; ventricular fibrillation; verapamil

Wave-front destabilization is the initiating event for ventricular fibrillation (VF), an arrhythmia that underlies most of the ≈335 000 sudden cardiac deaths per year in the United States.[1] Destabilization of wave fronts and the subsequent initiation of reentrant excitation can result from both intrinsic and dynamical heterogeneity of ventricular refractoriness (see elsewhere[2,3] for reviews). Dynamical heterogeneity arises primarily from electrical restitution

Correspondence to Anna Gelzer, College of Veterinary Medicine, Cornell University, Ithaca, NY 14853. arg9@cornell.edu.
[*]Drs Gelzer and Koller contributed equally.

Disclosures: None.

properties, ie, the dependence of action potential duration (APD) and conduction velocity (CV) on the preceding diastolic interval (DI) and pacing history.[4–6]

Our group has demonstrated in a computer modeling study that in the presence of a steeply sloped APD restitution relation, the delivery of multiple premature stimuli produces spatial gradients of repolarization that can precipitate propagation failure.[7] Recently, Otani[8] developed a theory in which APD restitution interacts with CV restitution to produce this type of conduction block. The purpose of the present study was to determine whether the predictions generated by these computer models are relevant to the development of VF in canine myocardium in vivo. Our hypothesis was that maximizing dynamic heterogeneity by delivering a set of premature stimuli that cause conduction block in the computer model would suffice to predictably induce VF in vivo. We further tested this hypothesis by determining whether calcium channel blockade, which has been shown previously to suppress the development of VF in vitro by decreasing the slope of the APD restitution relation,[9,10] reduces spatial dispersion of refractoriness and the inducibility of VF in vivo.

Methods

Two separate sets of experiments were performed in 2 groups of beagle dogs (Marshall Farms, North Rose, NY), group A (n=8) and group B (n=3). Experiments conducted on group A were performed to test the predictions resulting from the empirical modeling studies of Fox et al,[7] namely that premature stimulus combinations such as the "short-long-short-short" combination induce conduction block. Because the results obtained in group A dogs agreed well with the predictions of Fox et al, a more rigorous set of experiments were conducted in group B dogs using the predictions generated by the detailed theoretical model of Otani.[8]

Premature Stimulus Intervals Theoretically Predicted to Produce Block

Group A—In the modeling study by Fox et al,[7] APD and CV restitution functions measured in canine ventricular myocardium in vitro were used to construct a 1-dimensional coupled-maps computer model. The model was used to generate predictions regarding which combinations of premature stimuli were most (and least) likely to induce conduction block. The combinations generated by the computer model were delivered to the dogs in group A, as described below, to test whether the predictions were accurate.

Group B—For these experiments, predictions regarding which combinations of premature stimuli were most (and least) likely to produce conduction block were generated using the theoretical model of Otani.[8] This model also relies on APD and CV restitution relations to generate predictions. Rather than use previously recorded in vitro data for the APD restitution relation as in the group A dogs, we measured APD restitution from each ventricle in vivo at the time of the study. Because CV restitution could not be measured in vivo, the CV restitution relation determined previously in vitro was used for the modeling.[7]

The predictions for this set of experiments were generated by running a coupled-maps model (Reference 8, Equations 17 through 19) using all possible combinations of ΔDI_2, ΔDI_3, ΔDI_4, and ΔDI_5 between 0 and 70 ms in 1-ms increments, where $\Delta DI_x = DI_x - DI_{min}$; DI_x is the DI preceding stimulus S_x for x=2, 3, 4, and 5; and DI_{min} is the shortest DI allowing conduction of the subsequent premature beat. The simulations generated the following: all combinations of ΔDI_2 and ΔDI_3 that produced block of the S_3 wave; all combinations of ΔDI_2, ΔDI_3, and ΔDI_4 that produced block of the S_4 wave; and the largest value of ΔDI_5 that produced block of the S_5 wave for every combination of ΔDI_2, ΔDI_3, and ΔDI_4.

Experimental Preparations

Animals in both experimental groups were prepared identically. Adult beagle dogs (2 to 3 years of age) of either sex (n=11) that weighed on average 12.5 kg (range, 6 to 18 kg) and were maintained on standard chow were used. General anesthesia was induced with pentobarbital (30 mg/kg bolus IV) and maintained by continuous-rate infusion at 7 $mg \cdot kg^{-1} \cdot h^{-1}$.[11] Animals were ventilated to maintain oxygen tension at >100 mm Hg, arterial oxygen saturation at >96%, and carbon dioxide tension at 35 to 42 mm Hg and were given intravenous lactated Ringer's solution to maintain hydration and electrolyte balance. Arterial blood pressure and ECGs were recorded continuously.

Monophasic action potentials (MAPs) were recorded from the right ventricular (RV) and left ventricular (LV) endocardium with MAP catheters (7F, EP Technologies Inc, San Jose, Calif) introduced through transfemoral venous and arterial access. Ventricular stimulation was performed through the MAP catheter using rectangular pulses of 2-ms duration at twice the diastolic threshold. Data were digitized at 1000 Hz with 12-bit resolution and were recorded on an electrophysiology recording system (Biopac Systems, Inc, Goleta, Calif). Filter settings were 0.05 Hz for high pass and 500 Hz for low pass. Data analysis was performed with custom-written analysis programs in the MATLAB language.

After measurements were taken during control conditions, each dog in group A was given verapamil at continuous-rate infusions of 0.1 $mg \cdot kg^{-1} \cdot h^{-1}$ (V_{lo}), 0.3 $mg \cdot kg^{-1} \cdot h^{-1}$ (V_{med}), and 1.0 $mg \cdot kg^{-1} \cdot h^{-1}$ (V_{hi}), with each dose preceded by a bolus dose of 0.1 mg/kg. Measurements were obtained at steady state and 30 minutes after each increase in dose.

At the end of the study, the dogs were euthanized with an intravenous injection of sodium pentobarbital. All experimental protocols and procedures were approved by the Institutional Animal Care and Use Committee of the Center for Animal Research and Education at Cornell University (Ithaca, NY).

Pacing Protocols

Three pacing protocols were used for the group A experiments: (1) a protocol to establish the effective refractory periods (ERPs) after delivery of 1 to 4 premature stimuli, (2) a protocol to establish APD restitution during constant pacing, and (3) a protocol to test whether the premature stimulus intervals predicted by the computer model–induced conduction block (CL_{VF}) induced VF.

For the first protocol, the dogs were paced at a cycle length of 400 ms for 8 beats, after which a single premature stimulus (S_2) was delivered. The premature stimulus was delivered at progressively shorter S_1S_2 intervals until S_2 failed to capture (S_1S_{2min}). The S_1S_2 interval was then set to S_1S_{2min}+40 ms, and an S_3 stimulus was delivered at progressively shorter S_2S_3 intervals until it failed to capture (S_2S_{3min}). The procedure was then repeated to find S_3S_{4min} and S_4S_{5min}.

For the second protocol, the dynamic pace-down protocol,[12] drive trains of 50 stimuli were delivered at a constant S_1S_1 interval. The S_1S_1 interval of each drive train was decreased by 20 ms starting at 340 ms until 2:1 block occurred or VF was induced, in which case the dogs were immediately defibrillated with 50 to 100 J.

In the third protocol, a set of 4 appropriately timed premature stimuli designed to maximize dynamically induced spatial heterogeneity of refractoriness (CL_{VF}), as predicted by the Fox et al[7] study, were delivered. The sequence of stimuli was as follows: S_1S_{2min}+5 ms, S_2S_{3min}+50 ms, S_3S_{4min}+5 ms, and S_4S_{5min}+5 to 10 ms.

For the group B experiments, a dynamic pace-down protocol was conducted, as in Group A. The APD and DI data subsequently were used to calculate an APD restitution function and predictions regarding which sequences of premature stimuli were expected to induce VF and which were not. Because the testing of thousands of stimulus combinations in an in vivo experiment was clearly impractical, we took the following approach. Each premature stimulus from each combination tried was categorized according to whether the preceding DI was short (S) (ΔDI between 0 and 5 ms), intermediate (I) (ΔDI between 5 and 40 ms), or long (L) (ΔDI between 40 and 60 ms). The DI_{min} values used to calculate the ΔDI were determined separately for each combination of the preceding stimuli. Subsequently, stimulus combination categories were formed. For example, the SLSS category contains all combinations of stimuli for which ΔDI_2, ΔDI_4, and ΔDI_5 are between 0 and 5 ms and ΔDI_3 is between 40 and 60 ms. We attempted to test all 4 two-premature-stimuli combination categories, all 8 three-stimuli categories, and 14 of 16 possible categories involving 4 premature stimuli.

Determination of the APD Restitution Function

The APD restitution relation was determined by plotting APD (measured at 95% of repolarization [APD_{95}]) as a function of the preceding DI of the last action potential at each paced cycle length.[12] For the group A experiments, the maximum slope of the restitution relation was determined using a 4-parameter, sigmoidal function of the form $APD=a+b/\{1+\exp[-(DI-c)/d]\}$. For the group B dogs, the restitution relation was fit by solving the standard nonlinear least-squares problem using the functional form $APD=a+b\times\exp(-DI/c)$.

Interventricular Conduction Time and Dispersion

The conduction time (CT) between the RV and LV during the dynamic restitution protocol (ΔCT) was determined for group A dogs. ΔCT was defined as the maximum difference in RV to LV CT during stimulation at the longest and shortest cycle lengths of the dynamic restitution protocol. ΔCT was used as a surrogate parameter for CV, which could not be determined directly because the conduction path length between RV and LV MAP recording sites was not known. As an index of spatial dispersion of refractoriness, the sum of the difference in APD between the RV and LV of all premature impulses delivered at CL_{VF} (APD_{diff}) was determined. The APD restitution relation, ΔCT, APD_{diff}, and VF inducibility were assessed under control conditions and 30 minutes after administration of each dose of verapamil in group A dogs.

Statistical Analysis

In group A dogs, we used a linear mixed-effect model with dog as a random effect to assess the dependence of hemodynamic and electrophysiological parameters on verapamil dosage. We coded the control, low, medium, and high doses as a categorical factor and report the significance of the factor as a whole. We note that the mean responses for these factors all exhibit a monotonic relationship to dose level. We report the absolute value, presented as mean ±SEM, and the probability value for the factor. In group B dogs, we applied a likelihood-ratio test to logistic regression to assess the significance of the association between our theoretical predictions to induce VF and the outcome in the experiments. All statistical analyses were performed with JMP version 7 (SAS Institute Inc, Cary, NC). A value of $P<0.05$ was considered statistically significant.

The authors had full access to and take responsibility for the integrity of the data. All authors have read and agree to the manuscript as written.

Results

Induction of VF In Vivo With Dynamic Premature Stimulation

For the group A experiments, the theory predicted that the highest incidence of local conduction block should occur for (1) an S_1S_2 interval very close to S_1S_{2min}, (2) an S_2S_3 interval 50 ms longer than S_2S_{3min}, (3) an S_3S_4 interval very close to S_3S_{4min} and, (4) an S_4S_5 interval 5 to 10 ms longer than S_4S_{5min}. As shown in Table 1, delivery of this SLSS pattern (CL_{VF}) resulted in induction of VF in all 12 trials of group A dogs under baseline conditions. We also tested combinations of S_2 through S_5 sequences that should not, as predicted by the computer model, lead to local conduction block (CL_{NoVF}). VF was not inducible with these premature stimulus combinations in 6 of 9 trials (Table 1).

Delivery of CL_{VF} resulted in discordant APD alternans between RV and LV. As shown in Figure 1A, a short-long-short-long MAP APD sequence at the site of stimulation (RV) was associated with an opposite long-short-long-short APD sequence at the MAP recording site in the LV, followed by VF. There was significant spatial dispersion of refractoriness between the 2 recording sites during premature stimulation, as evidenced by an APD_{diff} value of 153 ms for the example shown in Figure 1A.

In the group B experiments, there was excellent agreement between the theoretical predictions and the experimental results, as illustrated by Figures 2 through 4. Nearly all stimulus combinations predicted not to produce block did not cause VF, as evidenced by the large number of green disks (indicating no induction of VF) appearing well away from the sequences predicted to cause VF in all 3 figures. Only 3 episodes of VF were not predicted by the theory, as represented by 1 red disk (indicating VF induction) located away from the sequences predicted to cause block in Figure 3 and 2 red disks in Figure 4. Conversely, 11 episodes of VF occurred when the theory indicated that VF was likely (1 episode in Figures 2, 3 episodes in Figure 3, and 7 episodes in Figure 4).

The mechanism for induction of conduction block is illustrated in Figure 5 with results from the theoretical model. As shown in Figure 5A, when the stimulus intervals were made as short as possible, the largest S_2–S_3 interval that produced block was 14 ms longer than the S_2 ERP (A). In contrast (Figure 5B), when the S_2–S_3 interval was longer (25 ms above ERP) while the S_1–S_2 and S_3–S_4 intervals were kept short (1 ms above ERP), a substantially longer S_4–S_5 interval was capable of producing block (25 ms above ERP).

The longer S_2–S_3 interval led to a substantial spatial gradient in the excitable period (the white, wedge-shaped region) between the S_2 and S_3 ERPs. This gradient was amplified and inverted during each subsequent action potential by the steep APD restitution function, yielding increasingly steep spatial gradients in the excitable periods between S_3 and S_4 and between S_4 and S_5. The latter was expressed largely through slow propagation of the S_4 wave back, which allowed the S_5 wave to catch up and run into it, even when the S_5 stimulus was 25 ms after the end of the S_4 ERP. The robustness of this mechanism likely accounts for the 100% success rate in producing VF with SLSx stimulus combinations, in contrast to the lower predicted and actual success rates in producing VF with a SSSx combination.

A statistical analysis was performed to determine whether an agreement existed between the experimental results and the theory. Each attempt to induce VF (n=105) was categorized by (1) the dog and (2) the ventricle in which the attempt was performed, (3) whether <25% or >25% of the stimulus combinations in the stimulus combination category used were predicted to produce block, and (4) whether VF induction was actually successful in the experiment. Table 2 summarizes these data. We then applied logistic regression to these data for the event of VF induction using dog, ventricle, and theoretical prediction as covariates. When the

likelihood-ratio test was applied to this method, neither the effect of dog (P=0.42) nor the effect of ventricle (P=0.25) was statistically different from 0. However, the effect of the theoretical prediction was significantly different from 0 (P<0.0001). The coefficient of prediction was 2.2.

Effects of Verapamil on Inducibility of VF

Tables 3 and 4 summarize the effects of verapamil on selected hemodynamic and electrophysiological parameters. The statistical analysis using a linear mixed-effect model yielded a probability value for the overall effect of dose. As Table 3 shows, verapamil significantly decreased arterial blood pressure and spontaneous heart rate and prolonged atrioventricular CT (as reflected by prolongation of the PR interval) as the dosage was increased. MAP recordings had a more triangular shape during verapamil infusion, which was associated with a significant prolongation of steady-state APD_{95} during constant pacing at a cycle length of 400 ms.

Verapamil significantly reduced the maximum slope of the dynamic APD restitution relation of the left ventricle and decreased the maximum difference in RV and LV CTs during stimulation at long and short cycle lengths (ΔCT). The changes in restitution parameters were associated with a tendency toward decreased spatial heterogeneity of refractoriness (APD_{diff}), but changes in the latter did not reach statistical significance (Table 4). In addition, inducibility of VF with CL_{VF} was reduced in a dose-dependent fashion by verapamil (Table 1).

An example of simultaneous MAP recordings from RV and LV during high-dose verapamil infusion and delivery of CL_{VF} is shown in Figure 1B. Compared with control conditions (Figure 1A), there was no discordant alternans between the RV and LV, and the duration of the premature action potentials was more uniform, as reflected by a markedly decreased APD_{diff} value of 32 ms. VF was not inducible by delivery of CL_{VF} during high-dose verapamil infusion in this dog.

Discussion

New Findings

In this study, we demonstrated in a computer model that maximizing dynamically induced spatial dispersion of refractoriness most often led to conduction block after a premature stimulus pattern of short-long-short-short. The predictions from the computer model with respect to which patterns of premature stimulation would cause conduction block were tested in canine myocardium in vivo. Delivery of CL_{VF}, predicted by the computer model to cause block, resulted in discordant APD alternans, followed by VF induction. Delivery of a premature stimulus combination that did not produce conduction block in the computer model typically did not induce VF in vivo.

A second important finding of this study is that modulation of APD restitution parameters via calcium channel blockade reduced spatial dispersion of repolarization and thereby reduced VF inducibility after premature stimulation. Verapamil reduced the slope of the APD restitution relation and decreased the magnitude of APD alternans, effects that inhibited the development of spatially discordant alternans and inducible VF. This result is in agreement with our previous in vitro studies[9] and earlier work demonstrating reduced MAP alternans in canine hearts in vivo after verapamil infusion.[13]

Significance of APD and CV Restitution for the Initiation of Wave Break

Wave break, thought to be an important cause of VF, may be caused by preexisting heterogeneities such as anatomic obstacles or regions of prolonged refractoriness. However, theoretical studies predict that wave break can arise purely on a dynamic basis secondary to spontaneous wavelength oscillations.[3–5] These oscillations develop because of fundamental restitution properties of the myocardium, namely that APD shortens and CV slows progressively as the pacing rate is increased. If the pacing rate is rapid enough to engage CV restitution, then successive waves will decelerate or accelerate, depending on how close they are to the wave back of the preceding wave, thereby causing spatially heterogeneous oscillations in wavelength that result in discordant APD alternans.[14–17]

Our computer model demonstrates that a short-long-short APD sequence at the site of premature stimulation is associated with a long-short-long sequence at the opposite end of the fiber. Discordant APD alternans enhances spatial dispersion of refractoriness, which may eventually cause local conduction block because additional premature beats may impinge on the wave back of the preceding wave. The results obtained from the computer model subsequently were validated in vivo; the cycle lengths that caused conduction block in the computer model (CL_{VF}) were associated with discordant APD alternans and induction of VF.

Antifibrillatory Effects Through Modulation of Restitution Parameters

Experimental studies have demonstrated that drugs such as bretylium, verapamil, and diacetyl monoxime, which flatten APD restitution and thereby suppress APD alternans, have antifibrillatory effects in vitro.[9,10] It is important to note that although verapamil decreased the slope of the dynamic restitution relation in the present study in vivo, the slope was not decreased to <1 even at verapamil doses that had significant negative inotropic and dromotropic effects. Because the slope of the APD restitution relation remained >1 after verapamil infusion, APD alternans was not eliminated by verapamil. However, verapamil reduced the magnitude of APD alternans, which was reflected in a decrease in APD dispersion during premature stimulation and a corresponding decrease in the difference in CTs. It seems likely that the reduced spatial dispersion of refractoriness prevented the development of discordant APD alternans, which, in turn, prevented conduction block and the initiation of VF. However, detailed mapping studies of the ventricles would be required to confirm this hypothesis and to eliminate the possibility that verapamil prevented the induction of VF by some other mechanism such as suppression of triggered activity.

Implications

Our study provides additional mechanistic insights for the well-recognized clinical observation that induction of rapid ventricular tachycardia and VF is often preceded either by a long-short-long[18] or a short-short-short sequence of ventricular premature beats.[19] Because of APD and CV restitution properties, a short-long-short sequence of premature beats maximizes spatial dispersion of refractoriness by inducing discordant APD alternans, which may eventually result in local conduction block. Local conduction block, in turn, is a prerequisite for the initiation of reentrant arrhythmias.

Our results further suggest that suppression of discordant APD alternans by drugs that appropriately modulate APD and CV restitution parameters may be a promising antiarrhythmic strategy, recognizing that several events may be required for the induction and subsequent maintenance of VF. Here, we address only one of these events: Are the necessary ingredients present to block some portion of a propagating wave? Although wave block may be a necessary condition for creating wave break, it is not sufficient. Heterogeneity in the direction perpendicular to propagation also is required; otherwise, the entire wave would block at once and no wave break would occur. Accordingly, it is likely that the intrinsic heterogeneity of

refractoriness contributed to the onset of VF in our experiments. It therefore follows that suppression of intrinsic heterogeneity also would be expected to prevent the induction of VF, an expectation supported by previous studies in which postrepolarization refractoriness was shown to reduce both dispersion of refractoriness and the inducibility of VF.[19]

Study Limitations

The primary limitations of the study were related to the fact that we obtained MAP recordings from only 2 sites, 1 in each ventricle. Consequently, we were not able to map the sequence of activation, which prevented us from determining CV as opposed to CTs. In addition, we were not able to determine the site of local conduction block, which would have required high-resolution mapping of the propagation wave fronts in the RV and LV.

A more general limitation of the study is that it was conducted in normal beagle dogs in the absence of overt heart disease. Given that sudden cardiac death occurs most often in patients with heart disease, the relevance of the present results to patients at risk for sudden cardiac death remains to be established. However, recent demonstrations that APD restitution is steep in some ventricular regions and is associated with the development of APD alternans in patients who lack structural heart disease[20,21] and that the incidence and magnitude of alternans are greater in patients who do have structural heart disease[21] suggest that studies of dynamically induced APD heterogeneity in normal dogs are likely be relevant to the clinical situation. If so, circumstances that maximize dynamical heterogeneity may increase the risk for VF.

Clinical Perspective

Our study demonstrates a novel mechanism of induction of ventricular fibrillation in vivo in intact normal beagle dogs. This work may contribute to our understanding of the mechanisms leading to the development of ventricular fibrillation in the structurally normal heart. For example, in patients with idiopathic ventricular fibrillation, focal ectopic ventricular activity originating in the Purkinje network is thought to trigger the onset of ventricular fibrillation. Our work also may be clinically relevant to patients with channelopathies, ie, long-QT syndrome, in which typically a short-long-short sequence of premature stimuli induces ventricular tachycardia and fibrillation. We showed in our study that such specific patterns (called CL_{VF}, cycle lengths inducing VF) can indeed lead to ventricular fibrillation by creating conduction block and wave break, depending on the restitution properties of the action potential duration and conduction velocity. In that regard, a potential therapeutic application of our work is to specifically target the restitution parameters with drugs so that CL_{VF} would no longer lead to ventricular fibrillation. We showed that the calcium channel blocker verapamil exerts antifibrillatory effects by altering restitution parameters but not at clinically relevant dosages. However, we postulate that other drugs may prove to have antiarrhythmic effects by altering the restitution parameters of a patient and thus may prevent the induction of ventricular fibrillation rather than by suppressing the premature stimuli.

Acknowledgments

We thank I. Davydenko for assistance with data analysis and preparation of the manuscript.

Sources of Funding: This work was supported by a research grant from the Deutsche Forschungsgemeinschaft (Ko 1782/2 to Dr Koller), by a scientist development grant from the American Heart Association, Northeast Affiliate (Dr Gelzer), and by National Institutes of Health grant HL075515 (Drs Gilmour and Fox).

References

1. Heart disease and stroke statistics: 2007 update. Circulation 2007;115:e69–e171. [PubMed: 17194875]
2. Janse MJ, Rosen MR. History of arrhythmias. Handb Exp Pharmacol 2006;171:1–39. [PubMed: 16610339]
3. Weiss JN, Qu Z, Chen PS, Lin SF, Karagueuzian HS, Hayashi H, Garfinkel A, Karma A. The dynamics of cardiac fibrillation. Circulation 2005;112:1232–1240. [PubMed: 16116073]
4. Karma A. Electrical alternans and spiral wave breakup in cardiac tissue. Chaos 1994;4:461–472. [PubMed: 12780121]
5. Cao JM, Qu Z, Kim YH, Wu TJ, Garfinkel A, Weiss JN, Karagueuzian HS, Chen PS. Spatiotemporal heterogeneity in the induction of ventricular fibrillation by rapid pacing: importance of cardiac restitution properties. Circ Res 1999;84:1318–1331. [PubMed: 10364570]
6. Qu Z, Weiss JN, Garfinkel A. Cardiac electrical restitution properties and stability of reentrant spiral waves: a simulation study. Am J Physiol 1999;276:H269–H283. [PubMed: 9887041]
7. Fox J, Riccio ML, Drury P, Werthman A, Gilmour RF Jr. Dynamic mechanism for conduction block in heart tissue. New J Phys 2003:101.101–101.114.
8. Otani NF. Theory of action potential wave block at-a-distance in the heart. Phys Rev E Stat Nonlin Soft Matter Phys 2007;75(pt 1):021910. [PubMed: 17358370]
9. Riccio ML, Koller ML, Gilmour RF Jr. Electrical restitution and spatiotemporal organization during ventricular fibrillation. Circ Res 1999;84:955–963. [PubMed: 10222343]
10. Garfinkel A, Kim YH, Voroshilovsky O, Qu Z, Kil JR, Lee MH, Karagueuzian HS, Weiss JN, Chen PS. Preventing ventricular fibrillation by flattening cardiac restitution. Proc Natl Acad Sci U S A 2000;97:6061–6066. [PubMed: 10811880]
11. Lumb, WV.; Jones, EW. Injectable anesthetics. In: Thurmon, JC.; Tranquilli, WJ.; Benson, GJ., editors. Veterinary Anesthesia. 3rd. Baltimore, Md: Williams and Wilkins; 1996. p. 218-223.
12. Koller ML, Riccio ML, Gilmour RF Jr. Dynamic restitution of action potential duration during electrical alternans and ventricular fibrillation. Am J Physiol 1998;275:H1635–H1642. [PubMed: 9815071]
13. Hirayama Y, Saitoh H, Atarashi H, Hayakawa H. Electrical and mechanical alternans in canine myocardium in vivo: dependence on intracellular calcium cycling. Circulation 1993;88:2894–2902. [PubMed: 8252703]
14. Qu Z, Garfinkel A, Chen PS, Weiss JN. Mechanisms of discordant alternans and induction of reentry in simulated cardiac tissue. Circulation 2000;102:1664–1670. [PubMed: 11015345]
15. Watanabe MA, Fenton FH, Evans SJ, Hastings HM, Karma A. Mechanisms for discordant alternans. J Cardiovasc Electrophysiol 2001;12:196–206. [PubMed: 11232619]
16. Fox JJ, Riccio ML, Hua F, Bodenschatz E, Gilmour RF Jr. Spatiotemporal transition to conduction block in canine ventricle. Circ Res 2002;90:289–296. [PubMed: 11861417]
17. Pastore JM, Laurita KR, Rosenbaum DS. Importance of spatiotemporal heterogeneity of cellular restitution in mechanism of arrhythmogenic discordant alternans. Heart Rhythm 2006;3:711–719. [PubMed: 16731476]
18. El-Sherif N, Gough WB, Restivo M. Reentrant ventricular arrhythmias in the late myocardial infarction period: mechanism by which a short-long-short cardiac sequence facilitates the induction of reentry. Circulation 1991;83:268–278. [PubMed: 1984885]
19. Koller BS, Karasik PE, Soloman AJ, Franz MR. The relationship between repolarization and refractoriness during programmed electrical stimulation in the human right ventricle: implications for ventricular tachycardia induction. Circulation 1995;91:2378–2384. [PubMed: 7729024]
20. Nash MP, Mourad A, Clayton RH, Sutton PM, Bradley CP, Hayward M, Paterson DJ, Taggart P. Evidence for multiple mechanisms in human ventricular fibrillation. Circulation 2006;114:536–542. [PubMed: 16880326]
21. Koller ML, Maier SK, Gelzer AR, Bauer WR, Meesmann M, Gilmour RF Jr. Altered dynamics of action potential restitution and alternans in humans with structural heart disease. Circulation 2005;112:1542–1548. [PubMed: 16157783]

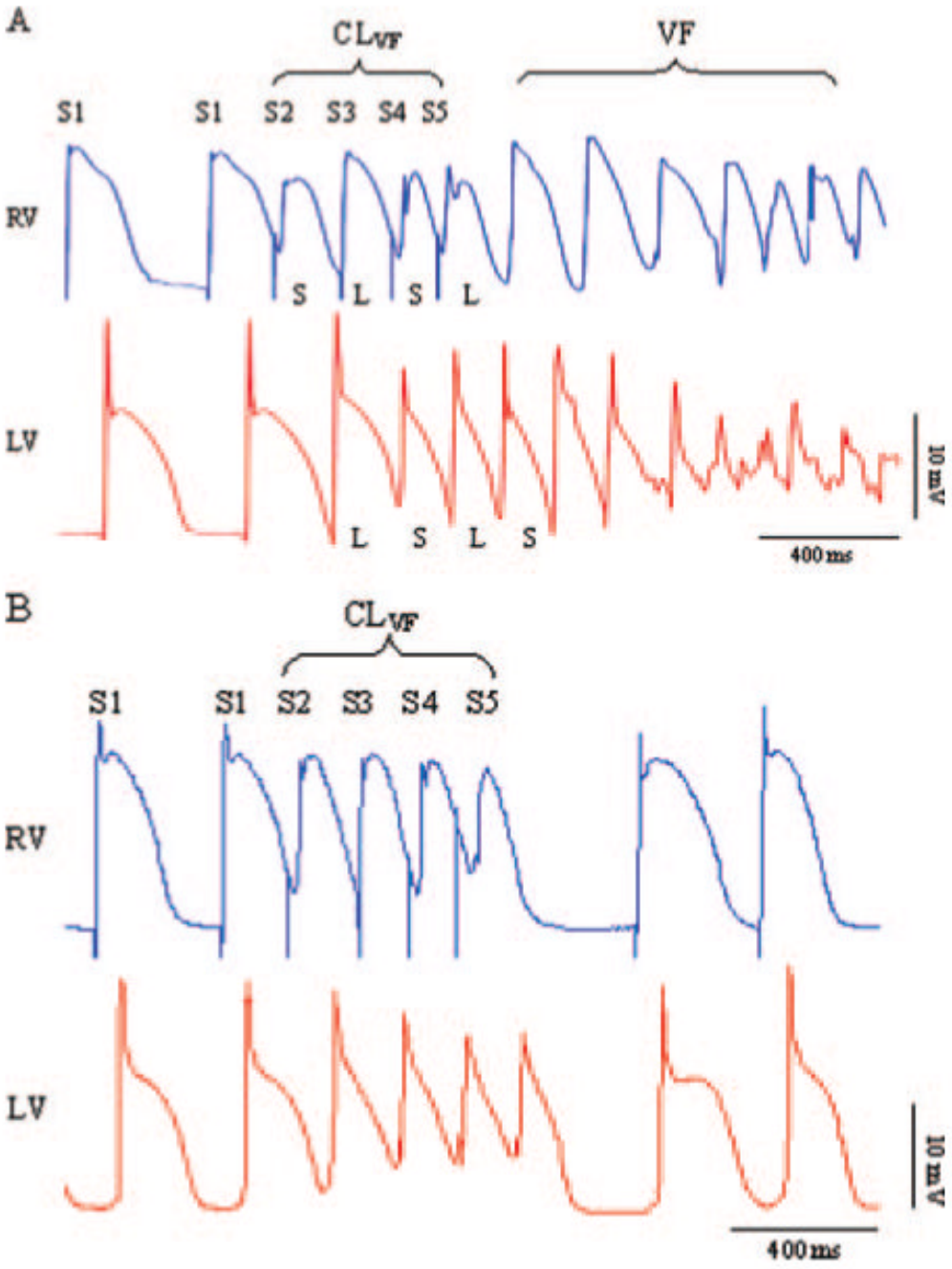

Figure 1.

Simultaneous MAP recordings from RV and LV endocardium. A, An example of VF induction by delivery of CL_{VF} in the RV. Note the discordant APD alternans between the RV and LV of the 4 premature action potentials (S_2 through S_5), which is followed by VF. APD_{diff} was 153 ms in this example. B, Delivery of CL_{VF} in the same dog but during high-dose verapamil infusion. Note the relatively uniform duration of the premature action potentials and the absence of discordant APD alternans. APD_{diff} was reduced to 32 ms, and VF was not inducible by delivery of CL_{VF}.

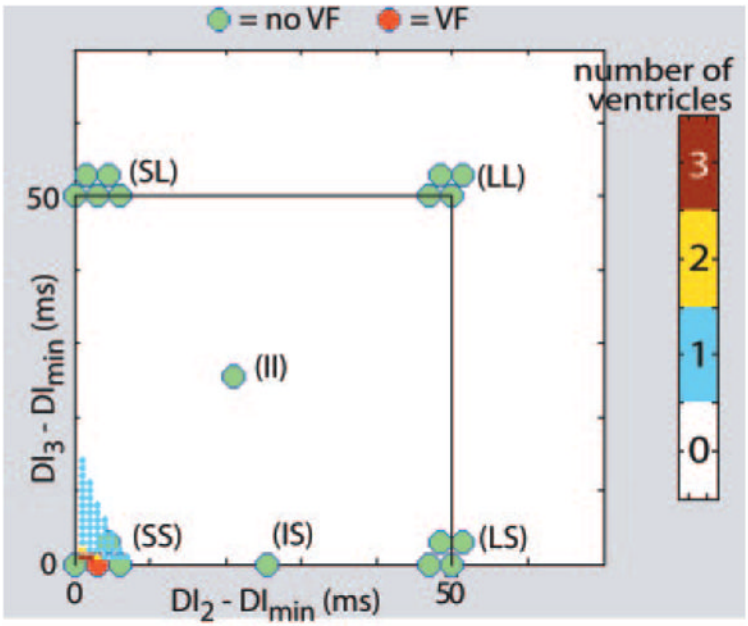

Figure 2.

Induction of VF with 2 premature stimuli: theoretical predictions and experimental results. The small, color-coded dots show the number of ventricles (of 5) in which all possible combinations of 2 premature stimuli were predicted to induce conduction block. The location of each dot defines a specific combination of premature stimuli through the coordinates of the dot, DI_2 and DI_3, relative to DI_{min}. The color of the dot designates the number of ventricles predicted to exhibit conduction block (see color bar, right) for that combination of premature stimuli. Note that conduction block was predicted to occur only for short-short (SS) sequences (all of the dots outside the SS region are white). In addition, even for SS intervals, only a few combinations were predicted to cause block in >1 ventricle (most of the dots in the SS region are blue). The color-coded disks show ventricles in which VF could (red) or could not (green) be induced experimentally with combinations of premature stimuli from various stimulus combination categories (made from short [S], intermediate [I], and long (L) intervals). The disks are clustered into groups, with each cluster labeled as 1 category (eg, SS, LS). Each disk within a cluster represents a ventricle that was subjected to a sequence of stimuli from that particular category. Note that, as predicted, all premature stimulus combinations other than SS failed to induce VF. Moreover, an SS combination induced VF in only 1 ventricle (of 4 tried), in good agreement with the theoretical predictions.

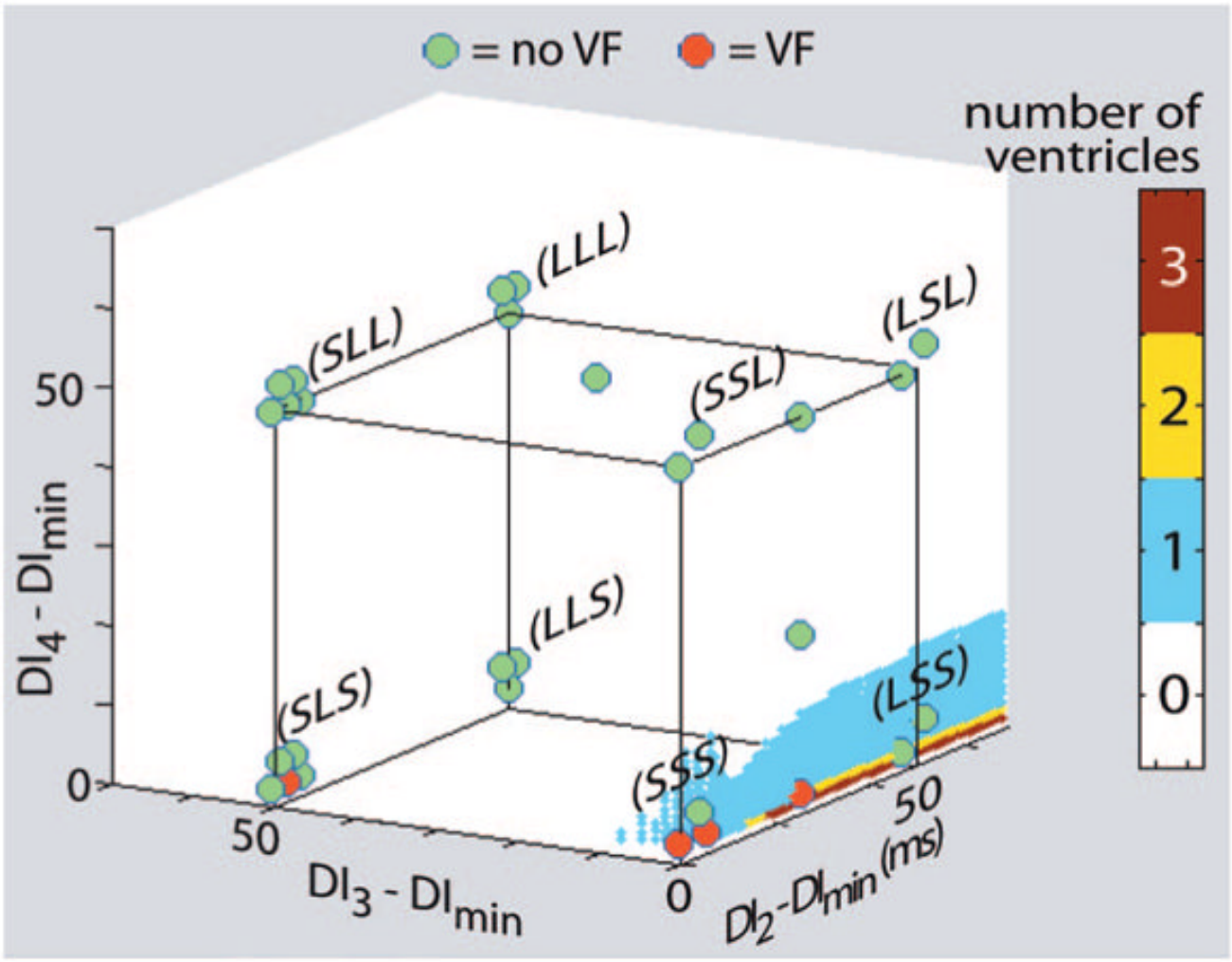

Figure 3.

Induction of VF with 3 premature stimuli: theoretical predictions and experimental results. As in Figure 2, the colors of the small dots (which appear to form a surface in the plot) indicate the number of ventricles (of 5) theoretically predicted to exhibit conduction block for various combinations of 3 premature stimuli. The color-coded disks within each cluster represent the number of ventricles in which VF could (red) or could not (green) be induced with combinations of premature stimuli from a particular stimulus combination category. Note that conduction block was predicted to occur primarily for SSS and LSS combinations and in only 1 of the 5 ventricles. With 1 exception (in the SLS category), VF induction occurred as predicted.

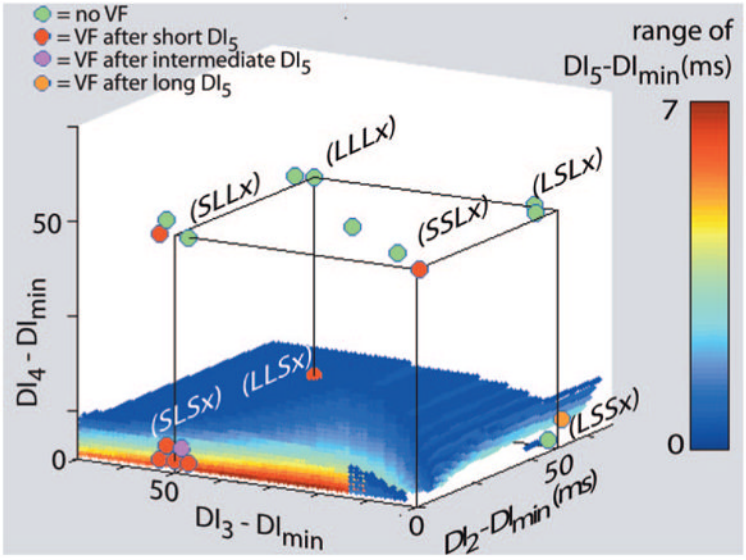

Figure 4.

Induction of VF with 4 premature stimuli: theoretical predictions and experimental results. The meaning of symbols in this plot is different from Figures 2 and 3. The small, color-coded dots show the range of DI_5 above DI_{min} for the fourth premature stimulus that is predicted to produce conduction block for various combinations of the first 3 premature stimuli. (Again, what appears to be a surface is actually composed of colored dots.) Each cluster of color-coded disks represents the 3 stimulus combination categories that have the same designation (ie, S, I, or L) for the first 3 premature stimuli and any one of S, I, or L as the designation for the fourth premature stimulus (x). The color of each disk indicates whether no combination of premature stimuli was able to induce VF (green) or whether a combination from the stimulus category with a short (S), intermediate (I), or long (L) fourth premature stimulus was able to induce VF (red, maroon, or orange, respectively). Note that 7 of 9 VF inductions were predicted by the theory and that, when conduction block was predicted, VF induction occurred in all cases except 1 (green disk at LSSx).

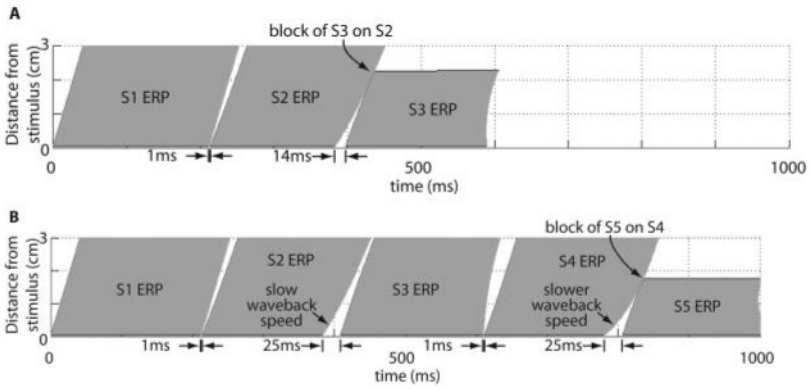

Figure 5.

A, Plot of the ERPs of S_1, S_2, and S_3 when the S_2 stimulus is delivered 1 ms after the S_1 ERP and the S_3 stimulus is delivered 14 ms after the S_2 ERP. This S_2S_3 interval is the largest such interval that produces block of the S_3 wave (ie, if S_3 is delivered 15 ms after the S_2 ERP, block of S_3 does not occur). B, S_1 through S_5 ERPs as functions of time and distance for S_2 through S_5 stimuli delivered 1, 25, 1, and 25 ms above ERP.

Table 1

Effects of Low, Medium, and High Verapamil Doses on Inducibility of VF With the SLSS Stimulation Combination Category

	Pacing Protocol	VF Induced	VF Not Induced
Control	CL_{VF}	12/12	0/12
Control	CL_{NoVF}	3/9	6/9
Verapamil low	CL_{VF}	5/8	3/8
Verapamil medium	CL_{VF}	4/8	4/8
Verapamil high	CL_{VF}	1/8	7/8

Results are expressed as number of events/number of trials; n=8 dogs. CL_{VF}: S_1S_1=400 ms, S_1S_2=S_1S_{2min}+5 ms, S_2S_3=S_2S_{3min}+40 ms, S_3S_4=S_3S_{4min}+5 ms, S_4S_5=S_4S_{5min}+5 to 10 ms. CL_{NoVF}: S_1S_1=400 ms, S_1S_2=S_1S_{2min}+40 ms, S_2S_3=S_2S_{3min}+40 ms, S_3S_4=S_3S_{4min}+40 ms, S_4S_5=S_4S_{5min}+5 ms.

Table 2

Percentage of Stimulus Combination Categories That Did or Did Not Produce VF in 2 Divisions of Stimulus Combination Categories Defined by the Fraction of Combinations in Each Category That Was Predicted Theoretically to Yield Conduction Block

	Theoretical Prediction	
Experimental Outcome	**<25% of Combinations Block, %**	**>25% of Combinations Block, %**
VF was inducible	8 (8/97)	75 (6/8)
VF could not be induced	92 (89/97)	25 (2/8)

Numbers in parentheses indicate the number of categories (trials) for which VF could or could not be induced.

Table 3

Effects of Dosage (Coded as Control, Low, Medium, and High) of Verapamil on Hemodynamic and Electrophysiological Parameters

	Control	V_{lo}	V_{med}	V_{hi}	*P*
BP_{syst}, mm Hg	164±8	142±7	131±9	129±10	0.0375
BP_{diast}, mm Hg	98±8	82±8	71±5	59±7	0.038
BP_{mean}, mm Hg	127±6	105±8	96±6	93±7	0.0013
HR, bpm	140±6	105±4	97±5	83±5	<0.0001
PR, ms	94±8	119±7	147±9	207±10	<0.0001
APD_{95} RV, ms	214±4	223±9	238±9	238±8	0.0086
APD_{95} LV, ms	220±4	241±10	240±8	245±10	0.0371

BP indicates arterial blood pressure; HR, heart rate; PR, PR interval of the ECG; and APD_{95}, APD at 95% repolarization in the RV and LV during steady-state pacing at a cycle length of 400 ms. Data are mean±SEM. Probability values show significance of factor as a whole.

Table 4

Effects of Dosage of Verapamil (Coded as Control, Low, Medium, and High) on the Maximum Slope of the LV Dynamic Restitution Function, ΔCT, and APD_{diff}

	Control	V_{lo}	V_{med}	V_{hi}	*P*
APDR	1.44±0.13	1.22±0.07	1.07±0.06	1.06±0.06	0.0069
ΔCT, ms	19.6±2.6	17.2±2.4	11.5±2.0	6.1±1.2	0.0002
APD_{diff}, ms	99±16	94±12	82±15	66±13	0.329

APDR indicates APD restitution relation. Data are mean±SEM. Probability values show significance of factor as a whole.